Check for updates

LIMNOLOGY AND OCEANOGRAPHY
Letters

ASLO
Open Access

Limnology and Oceanography Letters 9, 2024, 796–805
© 2024 The Author(s). *Limnology and Oceanography Letters* published by Wiley Periodicals LLC on behalf of Association for the Sciences of Limnology and Oceanography.
doi: 10.1002/lol2.10442

LETTER

Arctic fishes reveal patterns in radiocarbon age across habitats and with recent climate change

Ashley E. Stanek[1]*, *Jonathan A. O'Donnell*[2], *Michael P. Carey*[1], *Sarah M. Laske*[1], *Xiaomei Xu*[3], *Kenneth H. Dunton*[4], *Vanessa R. von Biela*[1]

[1]U.S. Geological Survey, Alaska Science Center, Anchorage, Alaska, USA; [2]National Park Service, Arctic Network, Anchorage, Alaska, USA; [3]Department of Earth Systems Science, Keck Carbon Cycle AMS Facility, University of California Irvine, Irvine, California, USA; [4]University of Texas at Austin, Marine Science Institute, Port Aransas, Texas, USA

Scientific Significance Statement

As the Arctic warms and permafrost thaws, older carbon (hundreds to many thousands of years old) is released, which can contribute a substantial amount of energy to food webs. Yet, we do not know if older carbon is in the food eaten by aquatic animals or if it is becoming more available or important over time. In this study, we used fish as natural samplers of aquatic ecosystems and found older carbon was used most in freshwater food webs and least in marine food webs. We then compared our results to similar fish data from ~ 40 yr earlier and found that older carbon may be less important than in the past.

Abstract

Climate change alters the sources and age of carbon in Arctic food webs by fostering the release of older carbon from degrading permafrost. Radiocarbon (^{14}C) traces carbon sources and age, but data before rapid warming are rare and limit assessments over time. We capitalized on ^{14}C data collected ~ 40 years ago that used fish as natural samplers by resampling the same species today. Among resampled fish, those using freshwater food webs had the oldest ^{14}C ages (> 1000 yr BP), while those using marine food webs had the youngest ^{14}C ages (near modern). One migratory species encompassed the entire range of ^{14}C ages because juveniles fed in freshwater streams and adults fed in offshore marine habitats. Over ~ 40 yr, average ^{14}C ages of freshwater and marine feeding fish shifted closer to atmospheric values, suggesting a potential influence from "greening of the Arctic."

*Correspondence: astanek@usgs.gov

Associate editor: Kozue Nishida (GE)

Author Contribution Statement: AES, SML, and VRV conducted the field work collecting samples while AES prepared samples in the laboratory for analysis. XX conducted the laboratory radiocarbon analysis. All authors came up with the research questions and study design. AES conducted statistical analyses and created figures. AES and VRV prepared the original draft of the manuscript while JAO, MPC, SML, XX, KHD reviewed and edited the manuscript.

Data Availability Statement: Data used in this study and associated metadata have been published in the USGS Alaska Science Center data repository at https://doi.org/10.5066/P9DAFMJD (Stanek et al. 2022a).

Additional Supporting Information may be found in the online version of this article.

This is an open access article under the terms of the Creative Commons Attribution License, which permits use, distribution and reproduction in any medium, provided the original work is properly cited.

The Arctic is warming nearly four times faster than the global average (Rantanen et al. 2022) with implications for habitats and food webs. Sea ice loss, permafrost thaw, shoreline erosion, and earlier river break-up (Jorgenson et al. 2006; Günther et al. 2015; Jones et al. 2018; Onarheim et al. 2018) can change biological production by altering sources or availability of organic matter (OM), an important source of energy and nutrients to aquatic food webs (Fritz et al. 2017; Mann et al. 2022). Permafrost stores vast amounts of largely frozen and inert older carbon (hundreds to tens of thousands of years old), which can mobilize upon thaw (Schuur et al. 2015; Schwab et al. 2020). Terrestrial OM ages vary widely in Arctic ecosystems, from contemporary vegetation to ancient permafrost sources (e.g., > 40,000 yr BP). Any alteration of OM supply, composition, or degradation state has potential to influence productivity because Arctic waters are often oligotrophic and nutrient limited (e.g., nitrogen, phosphorus) (Guillemette et al. 2017; O'Donnell et al. 2020). Radiocarbon (^{14}C) traces older carbon (i.e., carbon depleted in ^{14}C content) use in food webs (Schell et al. 1982; Schell 1983; Bellamy and Bauer 2017; Arimitsu et al. 2018; O'Donnell et al. 2020). The ^{14}C tracer provides a robust approach for tracking older carbon in a rapidly changing climate and cryosphere.

Given recent permafrost degradation in the Arctic, we anticipate that additional older carbon is circulating through ecosystems and food webs now compared to ~ 40 yr ago. This comparative study considers how climate change mobilizes older carbon to freshwater, estuarine, and marine food webs. Here, we captured fish in Alaska's nearshore Beaufort Sea because estuaries are crossroads where fish from different habitats coexist as natural samplers of the carbon continuum from freshwater to marine food webs. By comparing ^{14}C content (fraction modern, $F^{14}C$) of fishes with diverse feeding histories we can assess whether older carbon contributes to their respective food webs, and if so, determine potential locations where older carbon is entering aquatic food webs.

Differences in $F^{14}C$ among fish habitats were evaluated by comparing $F^{14}C$ of fish that use varied aquatic habitats from mountain streams to open ocean (Thorsteinson and Love 2016). Change over time was inferred by comparing $F^{14}C$ in fish collected recently and ~ 40 yr prior (Schell et al. 1982; Schell 1983), providing a rare opportunity for comparison spanning several decades. Although sample sizes provided in Schell (1983) and Schell et al. (1982) are small ($n = 40$ fish) and limit the strength of comparisons, these are the only known ^{14}C data sets that predate rapid warming in the Arctic.

This study considers two major hypotheses. (1) Fish feeding in freshwater have older ^{14}C ages than fish feeding in marine systems because freshwater has greater interaction (e.g., high surface area to volume) with soils that are sources of Holocene- to Pleistocene-aged terrestrial OM. (2) Fish collected in 2017–2019 have older ^{14}C ages compared to those sampled in 1977–1982 (Schell et al. 1982; Schell 1983) due to increased mobilization of older carbon via recent warming effects on the cryosphere (Hood et al. 2009; Estop-Aragonés et al. 2020) and carbon-cycle processes (e.g., Davidson and Janssens 2006).

Methods

Fish muscle samples used in this study are a subset of those in Stanek et al. (2022b); detailed sample collection is described therein. Briefly, 10 fish species with varied feeding habitats were collected in four Alaskan Beaufort Sea lagoons during summers 2017–2019 (Fig. 1). Within each species, differences in body lengths were used in analysis because feeding habitats and diets change as fish grow. Sample sizes for ^{14}C analysis differed across species (Table 1) with more samples for species with variable habitat and/or dietary diversity.

^{14}C analysis was conducted at the W. M. Keck Carbon Cycle Accelerator Mass Spectrometer (AMS) facility at the University of California Irvine (Beverly et al. 2010). Freeze-dried epaxial muscle was combusted at 900°C in evacuated, sealed quartz tubes in the presence of CuO. Following cryogenic purification, CO_2 was reduced to graphite at 550°C using the sealed tube Zn reduction method (Xu et al. 2007). All ^{14}C values reported are corrected for mass-dependent isotope fractionation using the AMS online $\delta^{13}C$ measurements. Results are reported as $F^{14}C$ following Reimer et al. (2004); $F^{14}C$ defines the ^{14}C activity of the atmosphere in 1950 as modern (0) age at a value of 1. However, nuclear weapons testing dramatically increased the ^{14}C content in the atmosphere, almost doubling $F^{14}C$ around 1963 (Supporting Information Fig. S1, Hua et al. 2022). Following the ban on nuclear bomb testing, $F^{14}C$ decreased due to exchange with carbon pools in the ocean and biosphere, and more recently, dilution from fossil fuel-induced CO_2 input. The "bomb spike" allows for $F^{14}C$ values of biological samples to also be ≫1

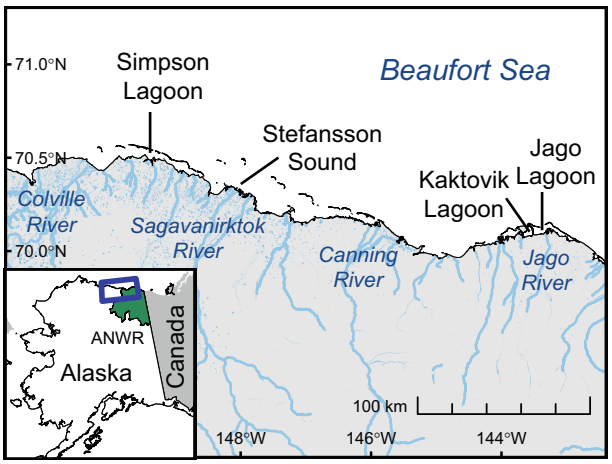


Fig. 1. The study area along the Beaufort Sea coast of Alaska where fish were collected from four lagoons in summers 2017–2019. The Arctic National Wildlife Refuge (ANWR) is identified in green.

23782242, 2024, 6, Downloaded from https://aslopubs.onlinelibrary.wiley.com/doi/10.1002/lol2.10442, Wiley Online Library on [13/03/2025]. See the Terms and Conditions (https://onlinelibrary.wiley.com/terms-and-conditions) on Wiley Online Library for rules of use; OA articles are governed by the applicable Creative Commons License

Table 1. Summary of radiocarbon content for groups of fish categorized by their food web and for individual species (with scientific and Iñupiaq names) sampled from Alaska's nearshore Beaufort Sea lagoons in summers 2017–2019. Radiocarbon content (mean ± SD) is expressed by fraction modern ($F^{14}C$), ^{14}C age (years before present), and $\Delta^{14}C$ (corrected for the year of sample collection, Stuiver and Polach 1977), along with the $F^{14}C$ range and the length range of individuals sampled. Species are ordered from marine residents to increasing diadromy and freshwater affinity. Length measurements (mm) are fork length for species with forked tails and total lengths for species with truncate or rounded tails (Stanek et al. 2022*a*).

	n	Length range (mm)	$F^{14}C$ range	$F^{14}C$ mean ± SD	^{14}C Age (yr BP)	$\Delta^{14}C_{corrected}$ (‰)
Food web						
Freshwater	57		0.7487–0.9789	0.8694 ± 0.0564	1124 ± 525	−137.7 ± 56.0
Mixture	36		0.8803–0.9729	0.9154 ± 0.0226	710 ± 197	−92.1 ± 22.4
Marine	78		0.8834–0.9960	0.9604 ± 0.0254	325 ± 214	−47.5 ± 25.2
Species						
Arctic Cod *Boreogadus saida*, Iqalugaq	10	91–219	0.9717–0.9958	0.9850 ± 0.0079	121 ± 64	−23.1 ± 7.8
Saffron Cod *Eleginus gracilis*, Uugaq	13	94–407	0.9226–0.9633	0.9447 ± 0.0129	457 ± 109	−63.1 ± 12.8
Arctic Flounder *Liposetta glacialis*, Nataaġnaq	7	93–234	0.8834–0.9394	0.9231 ± 0.0199	643 ± 175	−84.5 ± 19.8
Fourhorn Sculpin *Myoxocephalus quadricornis*, Kanayuq	7	70–224	0.8971–0.9620	0.9369 ± 0.0241	524 ± 208	−70.8 ± 24.0
Rainbow Smelt *Osmerus mordax*, Iłhuaġniq	7	96–265	0.9329–0.9780	0.9583 ± 0.0149	342 ± 125	−49.5 ± 14.8
Arctic Cisco *Coregonus autumnalis*, Qaaktaq	17	57–365	0.8933–0.9793	0.9495 ± 0.0254	416 ± 216	−58.3 ± 25.2
Humpback Whitefish *Coregonus pidschian*, Pikuktuuq	22	150–431	0.8803–0.9729	0.9046 ± 0.0199	805 ± 173	−102.8 ± 19.7
Broad Whitefish *Coregonus nasus*, Aanaakłiq	23	97–504	0.8254–0.9463	0.8712 ± 0.0342	1108 ± 312	−135.9 ± 33.9
Dolly Varden *Salvelinus malma*, Iqalukpik	48	125–589	0.7487–0.9960	0.9061 ± 0.0803	792 ± 731	−101.4 ± 79.7
Least Cisco *Coregonus sardinella*, Iqalusaaq	17	99–326	0.8676–0.9710	0.9407 ± 0.0233	491 ± 203	−67.0 ± 23.1

(Supporting Information Fig. S1). ^{14}C age represents the uncalibrated "apparent" average age of carbon in the sample.

Each fish was assigned to a food web using Stanek et al. (2022*b*) from dual stable isotope ($\delta^{13}C$ and $\delta^{15}N$) mixing models (MixSIAR, Stock et al. 2018) with two end-members representing freshwater (OM_{terr}) and marine (OM_{mar}) food webs (Supporting Information Fig. S2). Fish using > 67% OM_{terr} as their primary OM source were designated as "freshwater," "mixed" (i.e., estuarine) when using a mixture of OM_{terr} and OM_{mar} (33–67% OM_{terr}), and "marine" when using < 33% OM_{terr}. To test for differences in $F^{14}C$ among groups of fish with different food webs we used a Welch's ANOVA followed by a Games–Howell post hoc test. Arctic river ecosystems are dominated by allochthonous inputs of terrestrial carbon (Mann et al. 2016; O'Donnell et al. 2020). We did not identify or partition specific terrestrial OM sources (e.g., terrestrial vegetation), which was outside the bounds our study objectives. All statistical analyses were conducted using R (R Core Team 2024).

Generalized additive models (GAMs) determined relationships between $F^{14}C$ and length for each species as $F^{14}C = \alpha + f(\text{length}) + \varepsilon$; α is the model intercept, f is a smooth function of length measured in millimeters (Stanek et al. 2022*a*) with ≤ 4 df allowed, and ε is the residual error. GAMs were fit in the mcgv package (Wood 2011). Data used in this study are available in Stanek et al. (2022*a*).

Fish $F^{14}C$ was compared by time-period of collection (1977–1982 from Schell et al. 1982 and Schell 1983 or 2017–2019) and by species life history type (marine or diadromous) for a total of four groups. Only species sampled in both time periods were included in the temporal comparison. Marine residents included Arctic cod (*Boreogadus saida*, iqalugaq in Iñupiaq), Arctic flounder (*Liposetta glacialis*, nataaġnaq), and fourhorn sculpin (*Myoxocephalus quadricornis*,

23782242, 2024, 6, Downloaded from https://aslopubs.onlinelibrary.wiley.com/doi/10.1002/lol2.10442, Wiley Online Library on [13/03/2025]. See the Terms and Conditions (https://onlinelibrary.wiley.com/terms-and-conditions) on Wiley Online Library for rules of use; OA articles are governed by the applicable Creative Commons License

kanayuq). Diadromous fishes included Arctic cisco (*Coregonus autumnalis*, qaaktaq), humpback whitefish (*Coregonus pidschian*, Pikuktuuq), broad whitefish (*Coregonus nasus*, aanaakłiq), Dolly Varden (*Salvelinus malma*, iqalukpik), and least cisco (*Coregonus sardinella*, iqalusaaq). We corrected $F^{14}C$ values to account for the bomb curve as the difference from atmospheric values (fish $F^{14}C$–annual atmospheric $F^{14}C$ for collection year) so values of 0 denote carbon sourced entirely from atmospheric CO_2 during the year of collection. Bomb curve corrected $F^{14}C$ was compared among groups using Kruskall–Wallis ANOVA and Dunn's post hoc test.

Results

$F^{14}C$ of fish in Beaufort Sea lagoons from 2017 to 2019 spanned 0.7487 to 0.9960 (Table 1), reflecting average assimilated ^{14}C ages ranging from 2325 to 30 yr BP. $F^{14}C$ of fish differed among food webs (Fig. 2, $H_2 = 90.0$, $p < 0.001$; among pairs, all $p < 0.001$). On average, fish using freshwater food webs had the lowest $F^{14}C$ (mean ± SD; 0.8694 ± 0.0564, $n = 57$). Fish using marine food webs had the highest $F^{14}C$ (0.9604 ± 0.0254, $n = 78$), while fish in the mixed group had intermediate $F^{14}C$ (0.9154 ± 0.0226, $n = 36$) (Table 1).

Length was a significant ($\alpha < 0.01$) predictor of $F^{14}C$ for three species ($p < 0.001$, Fig. 3): Arctic cisco (adjusted $r^2 = 0.76$), Dolly Varden (adjusted $r^2 = 0.80$), and least cisco (adjusted $r^2 = 0.79$). Dolly Varden had the maximum and minimum $F^{14}C$ of all fish. $F^{14}C$ was lowest and increased rapidly with length for Dolly Varden ≤ 250 mm ($F^{14}C$ range = 0.7487–0.9651), while $F^{14}C$ was higher and increased little with length in Dolly Varden > 250 mm ($F^{14}C$ range = 0.9698–0.9960; Fig. 3). Among Arctic cisco the smallest and largest individuals had higher $F^{14}C$, while intermediate length fish had lower $F^{14}C$. Least cisco $F^{14}C$ was lowest in the smallest fish sampled and highest in the largest individuals sampled.

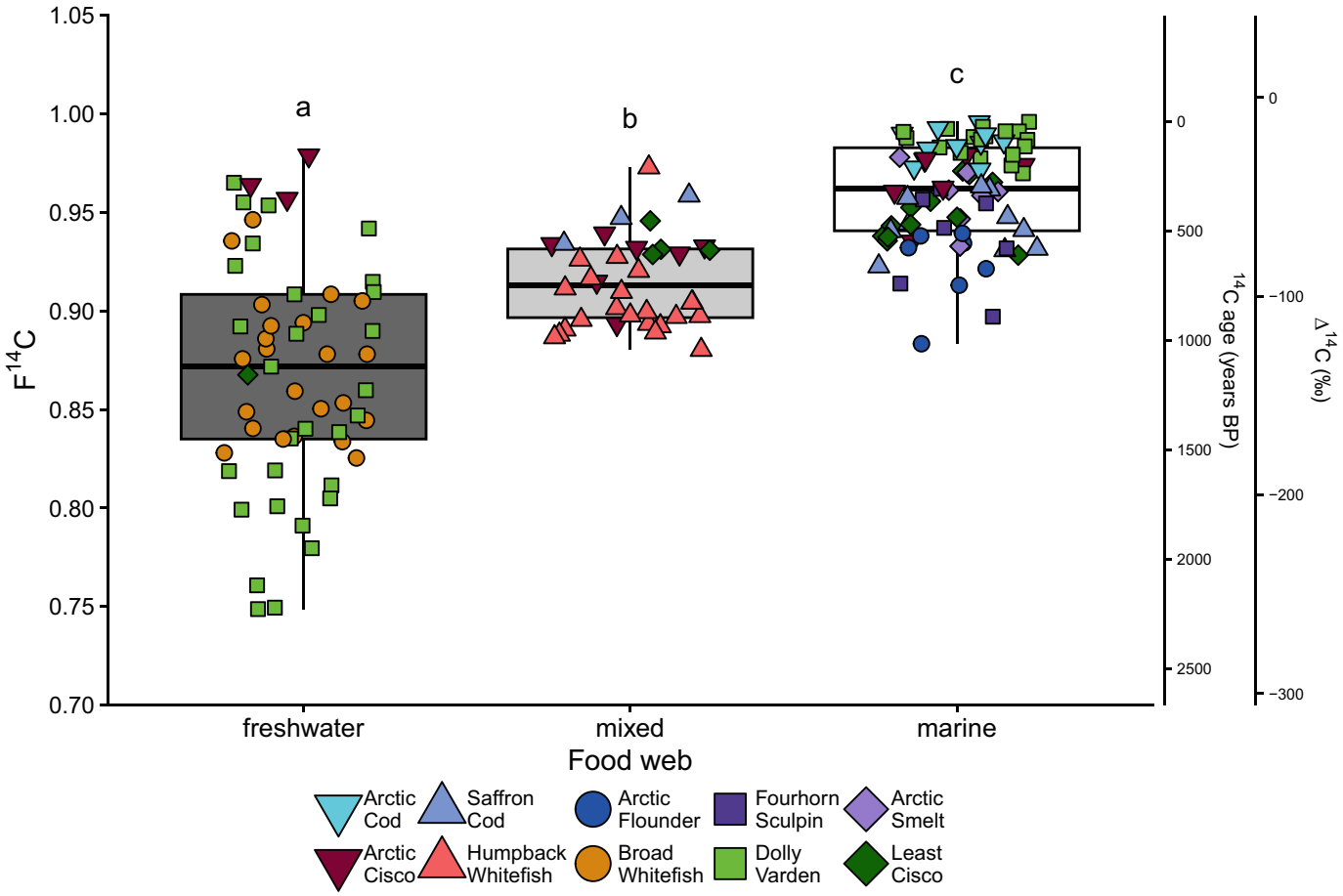


Fig. 2. Radiocarbon content (fraction modern, $F^{14}C$) grouped by food web for 10 species (color and shape) in the Beaufort Sea, Alaska, in summers 2017–2019. Boxplots identify the median (black line), the first and third quartiles (top and bottom of box), with whiskers showing the range in $F^{14}C$. Food webs for each individual were assigned using estimates of terrestrial organic matter (OM_{terr}) use as reported by Stanek et al. (2022b); "freshwater" individuals used > 67% OM_{terr}, "mixed" individuals used 33–67% OM_{terr}, while "marine" individuals used < 33% OM_{terr}. ^{14}C age (yr BP) and the corresponding $\Delta^{14}C$ values (‰, corrected for collection year) are shown on the right *y*-axes.

23782242, 2024, 6, Downloaded from https://aslopubs.onlinelibrary.wiley.com/doi/10.1002/lol2.10442, Wiley Online Library on [13/03/2025]. See the Terms and Conditions (https://onlinelibrary.wiley.com/terms-and-conditions) on Wiley Online Library for rules of use; OA articles are governed by the applicable Creative Commons License

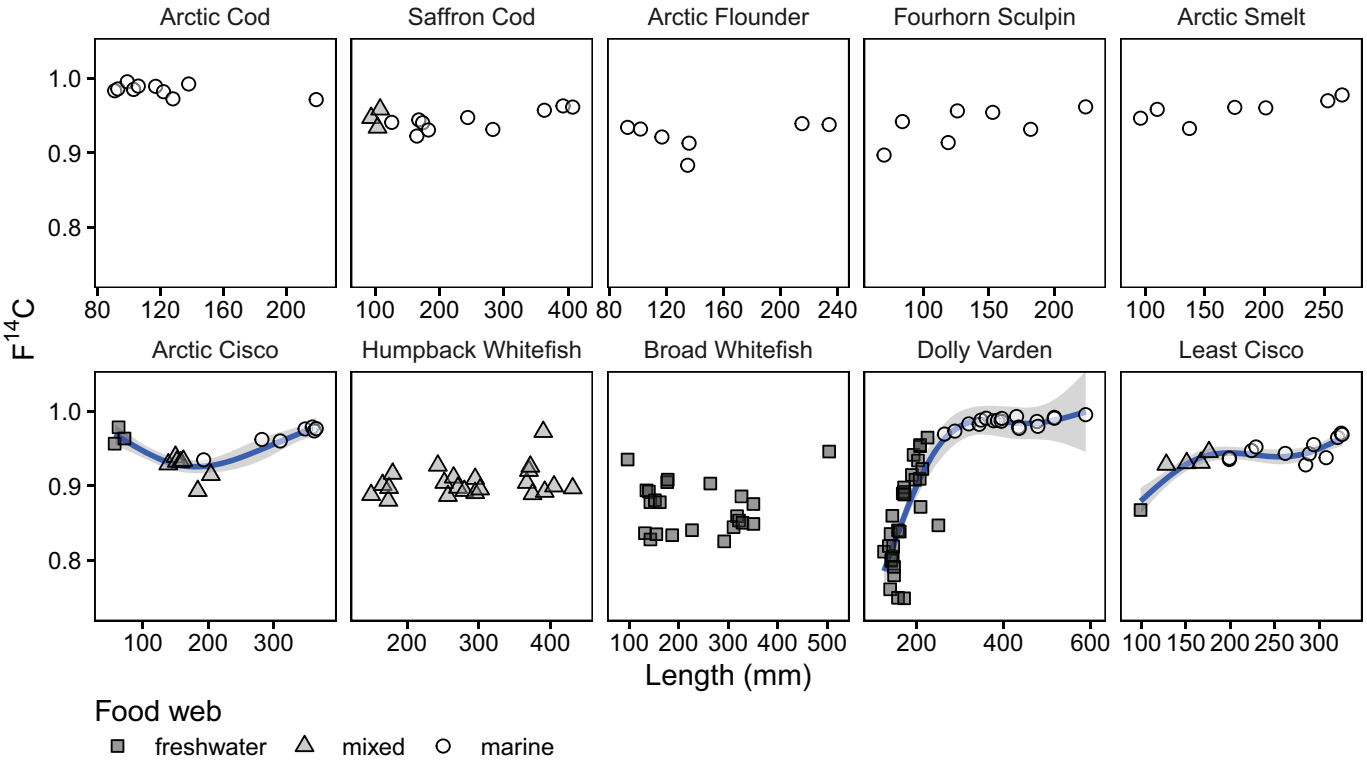


Fig. 3. Radiocarbon content (fraction modern, $F^{14}C$) of fish muscle by length (mm) for ten species in the Beaufort Sea, Alaska, in summers 2017–2019. Food webs for each individual were assigned using estimates of terrestrial organic matter (OM_{terr}) use as reported by Stanek et al. (2022*b*); "freshwater" individuals used > 67% OM_{terr} (dark gray squares), "mixed" individuals used 33–67% OM_{terr} (light gray triangles), while "marine" individuals used < 33% OM_{terr} (white circles). Generalized additive models (blue lines) are shown for species with a significant ($p \leq 0.01$) relationship between $F^{14}C$ and length.

Bomb curve corrected $F^{14}C$ of fish differed by time-period and life history type ($H_3 = 73.077$, $p < 0.001$; Fig. 4). Median bomb curve corrected $F^{14}C$ was lowest in fish from 1977 to 1982 regardless of life history type, intermediate for 2017–2019 diadromous fish, and highest among 2017–2019 marine fish (among pairs all adjusted $p < 0.05$; Fig. 4). Simply, $F^{14}C$ of fish shifted toward atmospheric $F^{14}C$ over time for both life histories.

Discussion

Fish captured in estuaries were excellent natural samplers of older carbon, exhibiting variation in ^{14}C age among species, within species, across food webs (freshwater, mixed, or marine), and between time periods providing key inferences about older carbon. Because of this natural variability in ^{14}C age among species and aquatic habitats, using fishes as natural samplers can help identify locations where future efforts aimed at understanding older carbon sources and carbon cycling are likely to be successful. We recommend locations where broad whitefish or juvenile Dolly Varden congregate in freshwater because they had the oldest ^{14}C ages (> 1000 yr BP). These locations likely have a complex mixture of modern and much older carbon sources (e.g., > 4000 yr BP) that result in the average millennial-aged carbon measured in these fish (O'Donnell et al. 2020). Sclerochronology approaches measuring ^{14}C in fish otoliths could provide a complimentary proxy of dissolved inorganic carbon ages (DIC) over space and time because otoliths are mostly derived from DIC (Solomon et al. 2006) while soft tissues used here reflect organic carbon.

Comparison of carbon age of fish among freshwater, mixed, and marine based food webs

We found the oldest ^{14}C ages for individuals that used freshwater food webs and the youngest ^{14}C ages for individuals that used marine food webs. Freshwater food webs of the Arctic comprise a broad range of OM sources, ranging from contemporary vegetation and organic-soil horizons (modern) to Holocene-aged glacial deposits (< 12,000 yr BP), to late Pleistocene loess deposits (> 12,000 yr BP) (Feng et al. 2013). Profiles of eroding Arctic coastlines show a layered gradient of ^{14}C ages in soils from modern at the surface to a few thousand years at the bottom of the active layer; deep within the permafrost, OM is much older, > 40,000 yr BP (Connolly et al. 2020; Bristol et al. 2021). Particulate organic carbon (POC), derived from glaciers, bank erosion, or thermal erosion of degrading permafrost, tends to be older than dissolved organic carbon

23782242, 2024, 6, Downloaded from https://aslopubs.onlinelibrary.wiley.com/doi/10.1002/lol2.10442, Wiley Online Library on [13/03/2025]. See the Terms and Conditions (https://onlinelibrary.wiley.com/terms-and-conditions) on Wiley Online Library for rules of use; OA articles are governed by the applicable Creative Commons License

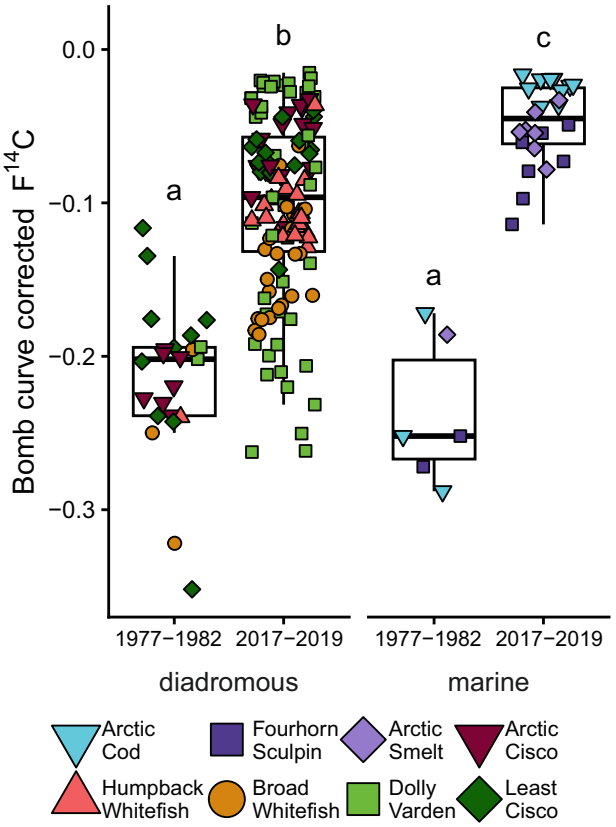


Fig. 4. A comparison of radiocarbon content (fraction modern, $F^{14}C$) of fishes corrected for the atmospheric bomb curve (fish $F^{14}C$—annual average atmospheric $F^{14}C$) from two time periods, 1977–1982 (Schell et al. 1982; Schell 1983) and 2017–2019 (this study) for diadromous and marine resident fishes. Only species (color and shape) that were sampled in both time periods are shown. Lowercase letters identify significantly different groups ($p < 0.05$). Boxplots identify the median (black line), the first and third quartiles (top and bottom of box), with whiskers extending to the range of values but no further than 1.5 times the interquartile range.

(DOC), which varies seasonally, with younger DOC prevalent during spring snowmelt and summer storm events and older DOC prevalent at winter baseflow (Guo et al. 2007; Estop-Aragonés et al. 2020). Both POC from glaciers and older DOC from sub-permafrost aquifers have been shown to fuel stream food webs (Fellman et al. 2015; O'Donnell et al. 2020). Marine OM ^{14}C ages vary with depth and salinity, with the oldest OM (5000–6000 yr BP) far offshore at depth (> 1000 m) and estuarine surface waters, used by our fish, expected to have the youngest ^{14}C ages given shallow depths and low salinities, although estuarine OM ages have not been directly measured (Druffel et al. 2017).

Comparison of fish carbon age between and within species

There was a greater contribution of older carbon to diadromous fish compared to marine residents that relied on younger, marine carbon sources throughout their lifespan. Fish often congregate by species and size because each group has different life history needs. For example, smaller fish consume benthic meiofauna and zooplankton, while larger fish shift toward epibenthic invertebrates or fish (von Biela et al. 2013; Laske et al. 2018). Among diadromous species, ^{14}C age was related to length in three species consistent with our understanding of each fishes' ecology. Diadromous fish of the Beaufort Sea hatch and overwinter in freshwater habitats but often feed in marine habitats during all (e.g., Arctic cisco) or some (e.g., Dolly Varden) life history phases (Brown et al. 2019; Carey et al. 2021). Dolly Varden ^{14}C ages, which were tightly linked to length, aligned with their migrations from groundwater-fed headwater streams (McCart 1980) to open ocean feeding (Gallagher et al. 2021). Freshwater food webs can receive older carbon from groundwater sources that flow through deeper active layers (Guo et al. 2007; Spencer et al. 2015; O'Donnell et al. 2020). Groundwater spring food webs can derive older carbon from a combination of > 1000 yr BP DOC and DIC that is assimilated by benthic biofilms at the base of food webs (O'Donnell et al. 2020). Dunmall et al. (2016) identified 35 groundwater springs draining to the Beaufort Sea used by Dolly Varden and any of these locations could be used by a future project aimed at understanding specific sources of older carbon to freshwater food webs.

Least cisco likely have a similar shift in ^{14}C with size as Dolly Varden, although data presented are less compelling because there was only one individual that retained an isotopic signal of freshwater feeding. Even with increased sample sizes, we expect ^{14}C changes with body size to be less dramatic for least cisco because they have a narrower migratory and feeding habitat range between low lying streams, rivers, and lakes to brackish river plumes in nearshore marine waters compared to Dolly Varden (Craig 1984; Thorsteinson and Love 2016). Least cisco are rarely found in headwater streams in the Brooks Range or full salt water like Dolly Varden (Craig 1984).

A different pattern of ^{14}C age and length was present for Arctic cisco likely because they have little to no freshwater feeding and originate in different rivers from Dolly Varden and least cisco (Craig 1984; Zimmerman et al. 2013). Arctic cisco spawn and hatch in Canada's Mackenzie River watershed, originating in the subarctic where abundant terrestrial vegetation captures relatively more modern carbon (DOC ^{14}C age 390–1440 yr BP) compared to Alaska's North Slope rivers (DOC ^{14}C age 2170–4960 yr BP; Guo et al. 2007). Thus, the smallest Arctic cisco retained isotopic values from feeding on modern terrestrial carbon in the Mackenzie River plume (von Biela et al. 2013). Older ^{14}C ages likely arose in intermediate length Arctic cisco because they feed and grow in the Alaskan nearshore Beaufort Sea, where freshwater run-off transports older carbon from Alaska's North Slope rivers to nearshore food webs (Dunton et al. 2006, 2012; Guo et al. 2007; Connolly et al. 2020). ^{14}C ages decrease again among the largest individuals likely because they

23782242, 2024, 6, Downloaded from https://aslopubs.onlinelibrary.wiley.com/doi/10.1002/lol2.10442, Wiley Online Library on [13/03/2025]. See the Terms and Conditions (https://onlinelibrary.wiley.com/terms-and-conditions) on Wiley Online Library for rules of use; OA articles are governed by the applicable Creative Commons License

transition to foods from marine food webs dominated by modern carbon (von Biela et al. 2013).

Comparison of fish carbon age across decades

A comparison of fish from 2017–2019 to 1977–1982 (Schell et al. 1982; Schell 1983) represents a unique, albeit coarse, opportunity to document shifts in age of carbon in fish of the Arctic over a multidecadal period of rapid climate change. When comparing ^{14}C age of fish over time (Schell et al. 1982; Schell 1983), we did not find support for our hypothesis that the average ^{14}C age reaching contemporary food webs was older due to mobilization of ancient carbon reservoirs with warming (e.g., permafrost carbon). Rather, our results suggest contemporary fish are supported by a higher proportion of modern carbon compared to fish collected ~ 40 yr prior. Changes in ^{14}C ages of fish over time are affected by the global carbon cycle, particularly the magnitude and directionality of ^{14}C fluxes among carbon reservoirs. While data presented here are unable to identify the cause of shifting ^{14}C ages, we provide three potential hypotheses that could explain our observation based on existing literature.

First, a shift in ^{14}C ages toward atmospheric values could occur due to a reversal in source–sink dynamics of atmospheric ^{14}C–CO_2 in recent decades. Before 1985, bomb-spike carbon in the atmosphere was taken up via terrestrial primary production and subsequently transferred to soils. Since 1985, some of this enriched ^{14}C has returned to the atmosphere due to warming-induced increases in soil heterotrophic respiration (Naegler and Levin 2009a,b). This release of bomb ^{14}C from terrestrial ecosystems to the atmosphere likely exerted a considerable and temporally variable masking effect on the anticipated older carbon signal that we expected to observe.

Second, the observation of shifting ^{14}C ages toward atmospheric values is consistent with "greening of the Arctic" in recent decades (Michelutti et al. 2005; Lewis et al. 2020; Myers-Smith et al. 2020). For instance, terrestrial net primary production and DOC export are highly correlated (Kicklighter et al. 2013) and studies have documented prevalent contemporary carbon in aquatic ecosystems of the Arctic (Elder et al. 2018; Garcia-Tigreros et al. 2023) likely reflecting the uptake of modern carbon by plants and subsequent transfer to streams and lakes. In addition, a lengthening of growing seasons and shorter winters may increase modern carbon availability to food webs. Schell (1983) argued that older carbon was particularly important in winter when pathways of modern carbon production via photosynthesis stalled due to lack of sunlight. Even with the possibility that contemporary carbon availability has increased more rapidly than aged carbon availability, ^{14}C ages from recent samples demonstrate that many freshwater fish still have detectable contributions from millennial-aged carbon sources.

Third, several studies indicate that mobilization of ancient permafrost carbon in contemporary aquatic ecosystems may be difficult to detect, due in part to the high bioavailability of permafrost DOC (Vonk et al. 2013; Mann et al. 2015). Permafrost DOC is comprised largely of low molecular-weight organic acids (e.g., acetate), that can be rapidly mineralized following thaw and release to aquatic ecosystems (Drake et al. 2015; Ewing et al. 2015; Spencer et al. 2015). Consequently, a significant fraction of ancient permafrost carbon may be rapidly transferred to the atmosphere before it can be taken up by aquatic food webs in higher-order rivers.

References

Arimitsu, M. L., K. A. Hobson, D. N. Webber, J. F. Piatt, E. W. Hood, and J. B. Fellman. 2018. Tracing biogeochemical subsidies from glacier runoff into Alaska's coastal marine food webs. Glob. Change Biol. **24**: 387–398. doi:10.1111/gcb.13875

Bellamy, A. R., and J. E. Bauer. 2017. Nutritional support of inland aquatic food webs by aged carbon and organic matter. Limnol. Oceanogr.: Lett. **2**: 131–149. doi:10.1002/lol2.10044

Beverly, R. K., W. Beaumont, D. Tauz, K. M. Ormsby, K. F. von Reden, G. M. Santos, and J. R. Southon. 2010. The keck carbon cycle AMS Laboratory, University of California, Irvine: Status report. Radiocarbon **52**: 301–309. doi:10.1017/S0033822200045343

Bristol, E. M., and others. 2021. Geochemistry of coastal permafrost and erosion-driven organic matter fluxes to the Beaufort Sea near Drew Point, Alaska. Front. Earth Sci. **8**: 598933. doi:10.3389/feart.2020.598933

Brown, R. J., M. B. Courtney, and A. C. Seitz. 2019. New insights into the biology of anadromous Dolly Varden in the Canning River, Arctic National Wildlife Refuge, Alaska. Trans. Am. Fish. Soc. **148**: 73–87. doi:10.1002/tafs.10122

Carey, M. P., V. R. von Biela, R. J. Brown, and C. E. Zimmerman. 2021. Migration strategies supporting salmonids in Arctic Rivers: A case study of Arctic Cisco and Dolly Varden. Anim. Migr. **8**: 132–143. doi:10.1515/ami-2020-0115

Connolly, C. T., M. B. Cardenas, J. W. McClelland, G. A. Burkart, and R. G. M. Spencer. 2020. Groundwater as a major source of dissolved organic matter to Arctic coastal waters. Nat. Commun. **11**: 1479. doi:10.1038/s41467-020-15250-8

Craig, P. C. 1984. Fish use of coastal waters of the Alaskan Beaufort Sea: A review. Trans. Am. Fish. Soc. **113**: 265–282. doi:10.1577/1548-8659(1984)113<265:FUOCWO>2.0.CO;2

Davidson, E. A., and I. A. Janssens. 2006. Temperature sensitivity of soil carbon decomposition and feedbacks to climate change. Nature **440**: 165–173. doi:10.1038/nature04514

Drake, T. W., K. P. Wickland, R. G. M. Spencer, D. M. McKnight, and R. G. Striegl. 2015. Ancient low-molecular-weight organic acids in permafrost fuel rapid

23782242, 2024, 6, Downloaded from https://aslopubs.onlinelibrary.wiley.com/doi/10.1002/lol2.10442, Wiley Online Library on [13/03/2025]. See the Terms and Conditions (https://onlinelibrary.wiley.com/terms-and-conditions) on Wiley Online Library for rules of use; OA articles are governed by the applicable Creative Commons License

carbon dioxide production upon thaw. Proc. Natl. Acad. Sci. USA **112**: 13946–13951. doi:10.1073/pnas.1511705112

Druffel, E. R. M., S. Griffin, C. S. Glynn, R. Benner, and B. D. Walker. 2017. Radiocarbon in dissolved organic and inorganic carbon of the Arctic Ocean. Geophys. Res. Lett. **44**: 2369–2376. doi:10.1002/2016GL072138

Dunmall, K. M., N. J. Mochnacz, C. E. Zimmerman, C. Lean, and J. D. Reist. 2016. Using thermal limits to assess establishment of fish dispersing to high-latitude and high-elevation watersheds. Can. J. Fish. Aquat. Sci. **73**: 1750–1758. doi:10.1139/cjfas-2016-0051

Dunton, K. H., T. Weingartner, and E. C. Carmack. 2006. The nearshore western Beaufort Sea ecosystem: Circulation and importance of terrestrial carbon in arctic coastal food webs. Prog. Oceanogr. **71**: 362–378. doi:10.1016/j.pocean.2006.09.011

Dunton, K. H., S. V. Schonberg, and L. W. Cooper. 2012. Food web structure of the Alaskan nearshore shelf and estuarine lagoons of the Beaufort Sea. Estuaries Coasts **35**: 416–435. doi:10.1007/s12237-012-9475-1

Elder, C. D., and others. 2018. Greenhouse gas emissions from diverse Arctic Alaskan lakes are dominated by young carbon. Nat. Clim. Change **8**: 166–171. doi:10.1038/s41558-017-0066-9

Estop-Aragonés, C., and others. 2020. Assessing the potential for mobilization of old soil carbon after permafrost thaw: A synthesis of ^{14}C measurements from the northern permafrost region. Glob. Biogeochem. Cycles **34**: e2020GB006672. doi:10.1029/2020GB006672

Ewing, S. A., J. A. O'Donnell, G. R. Aiken, K. Butler, D. Butman, L. Windham-Myers, and M. Z. Kanevskiy. 2015. Long-term anoxia and release of ancient, labile carbon upon thaw of Pleistocene permafrost. Geophys. Res. Lett. **42**: 10730–10738. doi:10.1002/2015GL066296

Fellman, J. B., E. Hood, P. A. Raymond, J. Hudson, M. Bozeman, and M. L. Arimitsu. 2015. Evidence for the assimilation of ancient glacier organic carbon in a proglacial stream food web. Limnol. Oceanogr. **60**: 1118–1128. doi:10.1002/lno.10088

Feng, X., and others. 2013. Differential mobilization of terrestrial carbon pools in Eurasian Arctic river basins. Proc. Natl. Acad. Sci. USA **110**: 14168–14173. doi:10.1073/pnas.1307031110

Fritz, M., J. E. Vonk, and H. Lantuit. 2017. Collapsing Arctic coastlines. Nat. Clim. Change **7**: 6–7. doi:10.1038/nclimate3188

Gallagher, C. P., M. B. Courtney, A. C. Seitz, E. V. Lea, and K. L. Howland. 2021. Ocean-entry timing and marine habitat-use of Canadian Dolly Varden: Dispersal among conservation, hydrocarbon exploration, and shipping areas in the Beaufort Sea. Estuar. Coast. Shelf Sci. **262**: 107609. doi:10.1016/j.ecss.2021.107609

Garcia-Tigreros, F., and others. 2023. Arctic-boreal lakes of interior Alaska dominated by contemporary carbon. Environ. Res. Lett. **18**: 124024. doi:10.1088/1748-9326/ad0993

Guillemette, F., T. S. Bianchi, and R. G. M. Spencer. 2017. Old before your time: Ancient carbon incorporation in contemporary aquatic foodwebs. Limnol. Oceanogr. **62**: 1682–1700. doi:10.1002/lno.10525

Günther, F., P. P. Overduin, I. A. Yakshina, T. Opel, A. V. Baranskaya, and M. N. Grigoriev. 2015. Observing Muostakh disappear: Permafrost thaw subsidence and erosion of a ground-ice-rich island in response to Arctic summer warming and sea ice reduction. Cryosphere **9**: 151–178. doi:10.5194/tc-9-151-2015

Guo, L., C. L. Ping, and R. W. Macdonald. 2007. Mobilization pathways of organic carbon from permafrost to arctic rivers in a changing climate. Geophys. Res. Lett. **34**: L13603. doi:10.1029/2007GL030689

Hood, E., J. Fellman, R. G. M. Spencer, P. J. Hernes, R. Edwards, D. Damore, and D. Scott. 2009. Glaciers as a source of ancient and labile organic matter to the marine environment. Nature **462**: 1044–1047. doi:10.1038/nature08580

Hua, Q., and others. 2022. Atmospheric radiocarbon for the period 1950-2019. Radiocarbon **64**: 723–745. doi:10.1017/RDC.2021.95

Jones, B. M., and others. 2018. A decade of remotely sensed observations highlight complex processes linked to coastal permafrost bluff erosion in the Arctic. Environ. Res. Lett. **13**: 115001. doi:10.1088/1748-9326/aae471

Jorgenson, M. T., Y. L. Shur, and E. R. Pullman. 2006. Abrupt increase in permafrost degradation in Arctic Alaska. Geophys. Res. Lett. **33**: L02503. doi:10.1029/2005GL024960

Kicklighter, D. W., D. J. Hayes, J. W. McClelland, B. J. Peterson, A. D. Mcguire, and J. M. Melillo. 2013. Insights and issues with simulating terrestrial DOC loading of Arctic river networks. Ecol. Appl. **23**: 1817–1836. doi:10.1890/11-1050.1

Laske, S. M., A. E. Rosenberger, M. S. Wipfli, and C. E. Zimmerman. 2018. Generalist feeding strategies in Arctic freshwater fish: A mechanism for dealing with extreme environments. Ecol. Freshw. Fish **27**: 767–784. doi:10.1111/eff.12391

Lewis, K. M., G. L. Van Dijken, and K. R. Arrigo. 2020. Changes in phytoplankton concentration now drive increased Arctic Ocean primary production. Science **369**: 198–202. doi:10.1126/science.aay8380

Mann, P. J., T. I. Eglinton, C. P. McIntyre, N. Zimov, A. Davydova, J. E. Vonk, R. M. Holmes, and R. G. M. Spencer. 2015. Utilization of ancient permafrost carbon in headwaters of Arctic fluvial networks. Nat. Commun. **6**: 7856. doi:10.1038/ncomms8856

Mann, P. J., and others. 2016. Pan-Arctic trends in terrestrial dissolved organic matter from optical measurements. Front. Earth Sci. **4**: 25. doi:10.3389/feart.2016.00025

Mann, P. J., and others. 2022. Degrading permafrost river catchments and their impact on Arctic Ocean nearshore processes. Ambio **51**: 439–455. doi:10.1007/s13280-021-01666-z

23782242, 2024, 6, Downloaded from https://aslopubs.onlinelibrary.wiley.com/doi/10.1002/lol2.10442, Wiley Online Library on [13/03/2025]. See the Terms and Conditions (https://onlinelibrary.wiley.com/terms-and-conditions) on Wiley Online Library for rules of use; OA articles are governed by the applicable Creative Commons License

McCart, P. J. 1980. *A review of the systematics and ecology of Arctic Char,* Salvelinus alpinus*, in the Western Arctic*. Canadian Technical Report of Fisheries and Aquatic Sciences. https://www.arlis.org/docs/vol1/DFO/TR/TR935.pdf

Michelutti, N., A. P. Wolfe, R. D. Vinebrooke, B. Rivard, and J. P. Briner. 2005. Recent primary production increases in arctic lakes. Geophys. Res. Lett. **32**: L19715. doi:10.1029/2005GL023693

Myers-Smith, I. H., and others. 2020. Complexity revealed in the greening of the Arctic. Nat. Clim. Change **10**: 106–117. doi:10.1038/s41558-019-0688-1

Naegler, T., and I. Levin. 2009*a*. Observation-based global biospheric excess radiocarbon inventory 1963-2005. J. Geophys. Res.: Atmos. **114**: D17302. doi:10.1029/2008JD011100

Naegler, T., and I. Levin. 2009*b*. Biosphere-atmosphere gross carbon exchange flux and the $\delta^{13}CO_2$ and $\Delta^{14}CO_2$ disequilibria constrained by the biospheric excess radiocarbon inventory. J. Geophys. Res.: Atmos. **114**: D17303. doi:10.1029/2008JD011116

O'Donnell, J. A., M. P. Carey, J. C. Koch, X. Xu, B. A. Poulin, J. Walker, and C. E. Zimmerman. 2020. Permafrost hydrology drives the assimilation of old carbon by stream food webs in the Arctic. Ecosystems **23**: 435–453. doi:10.1007/s10021-019-00413-6

Onarheim, I. H., T. Eldevik, L. H. Smedsrud, and J. C. Stroeve. 2018. Seasonal and regional manifestation of Arctic sea ice loss. J. Clim. **31**: 4917–4932. doi:10.1175/JCLI-D-17-0427.1

R Core Team. 2024. *R: A language and environment for statistical computing*. R Foundation for Statistical Computing, Vienna, Austria. https://www.R-project.org

Rantanen, M., A. Y. Karpechko, A. Lipponen, K. Nordling, O. Hyvärinen, K. Ruosteenoja, T. Vihma, and A. Laaksonen. 2022. The Arctic has warmed nearly four times faster than the globe since 1979. Commun. Earth Environ. **3**: 168. doi:10.1038/s43247-022-00498-3

Reimer, P. J., T. A. Brown, and R. W. Reimer. 2004. Discussion: Reporting and calibration of post-bomb ^{14}C data. Radiocarbon **46**: 1299–1304. doi:10.1017/S0033822200033154

Schell, D. M. 1983. Carbon-13 and carbon-14 abundances in Alaskan aquatic organisms: Delayed production from peat in arctic food webs. Science **219**: 1068–1071. doi:10.1126/science.219.4588.1068

Schell, D. M., P. J. Ziemann, D. M. Parrish, K. H. Dunton, and E. J. Brown. 1982. Foodweb and nutrient dynamics in nearshore Alaska Beaufort Sea waters. National Oceanographic and Atmospheric Administration, Outer Continental Shelf Environmental Assessment Program Final Reports 25. https://www.arlis.org/docs/vol1/OCSEAP2/Final/OCSEAP-Final-v25.pdf

Schuur, E. A. G., and others. 2015. Climate change and the permafrost carbon feedback. Nature **520**: 171–179. doi:10.1038/nature14338

Schwab, M. S., and others. 2020. An abrupt aging of dissolved organic carbon in large Arctic rivers. Geophys. Res. Lett. **47**: e2020GL088823. doi:10.1029/2020GL088823

Solomon, C. T., P. K. Weber, J. J. Cech Jr., B. L. Ingram, M. E. Conrad, M. V. Machavaram, A. R. Pogodina, and R. L. Franklin. 2006. Experimental determination of the sources of otolith carbon and associated isotopic fractionation. Can. J. Fish. Aquat. Sci. **63**: 79–89. doi:10.1139/f05-200

Spencer, R. G. M., P. J. Mann, T. Dittmar, T. I. Eglinton, C. McIntyre, R. M. Holmes, N. Zimov, and A. Stubbins. 2015. Detecting the signature of permafrost thaw in Arctic rivers. Geophys. Res. Lett. **42**: 2830–2835. doi:10.1002/2015GL063498

Stanek, A. E., V. R. von Biela, S. M. Laske, K. H. Dunton, M. P. Carey, and J. A. O'Donnell. 2022*a*. Nearshore fish isotope values, Beaufort Sea, Alaska, 2017–2019 (ver 2.0, January 2024): U.S. Geological Survey data release. doi:10.5066/P9DAFMJD

Stanek, A. E., V. R. von Biela, S. M. Laske, R. L. Taylor, and K. H. Dunton. 2022*b*. Barrier islands influence the assimilation of terrestrial energy in nearshore fishes. Estuar. Coast. Shelf Sci. **278**: 108094. doi:10.1016/j.ecss.2022.108094

Stock, B. C., A. L. Jackson, E. J. Ward, A. C. Parnell, D. L. Phillips, and B. X. Semmens. 2018. Analyzing mixing systems using a new generation of Bayesian tracer mixing models. PeerJ **6**: e5096. doi:10.7717/peerj.5096

Stuiver, M., and H. A. Polach. 1977. Discussion reporting of ^{14}C data. Radiocarbon **19**: 355–363. doi:10.1017/S0033822200003672

Thorsteinson, L. K., and M. S. Love [eds.]. 2016. *Alaska Arctic marine fish ecology catalog: U.S. Geological Survey Scientific Investigations Report 2016-5038 (OCS Study, BOEM 2016-048)*. U.S. Geological Survey. doi:10.3133/sir20165038

von Biela, V. R., C. E. Zimmerman, B. R. Cohn, and J. M. Welker. 2013. Terrestrial and marine trophic pathways support young-of-year growth in a nearshore Arctic fish. Polar Biol. **36**: 137–146. doi:10.1007/s00300-012-1244-x

Vonk, J. E., and others. 2013. High biolability of ancient permafrost carbon upon thaw. Geophys. Res. Lett. **40**: 2689–2693. doi:10.1002/grl.50348

Wood, S. N. 2011. Fast stable restricted maximum likelihood and marginal likelihood estimation of semiparametric generalized linear models. J. R. Stat. Soc. Ser. B Stat. Methodol. **73**: 3–36. doi:10.1111/j.1467-9868.2010.00749.x

Xu, X., S. E. Trumbore, S. Zheng, J. R. Southon, K. E. McDuffee, M. Luttgen, and J. C. Liu. 2007. Modifying a sealed tube zinc reduction method for preparation of AMS graphite targets: Reducing background and attaining high precision. Nucl. Instrum. Methods Phys. Res. B: Beam Interact. Mater. Atoms **259**: 320–329. doi:10.1016/j.nimb.2007.01.175

Zimmerman, C. E., A. M. Ramey, S. M. Turner, F. J. Mueter, S. M. Murphy, and J. L. Nielsen. 2013. Genetics,

23782242, 2024, 6, Downloaded from https://aslopubs.onlinelibrary.wiley.com/doi/10.1002/lol2.10442, Wiley Online Library on [13/03/2025]. See the Terms and Conditions (https://onlinelibrary.wiley.com/terms-and-conditions) on Wiley Online Library for rules of use; OA articles are governed by the applicable Creative Commons License

recruitment, and migration patterns of Arctic cisco (*Coregonus autumnalis*) in the Colville River, Alaska, and Mackenzie River, Canada. Polar Biol. **36**: 1543–1555. doi:10.1007/s00300-013-1372-y

Acknowledgments

We greatly appreciate the knowledge shared by the people of Kaktovik during field sampling. We could not have conducted this work without the expertise of RV *Proteus* captains Ted Dunton and John Dunton. We thank Cathy Coon, Sean Burril, Dan Donnelly, Cody Dawson, Arctic National Wildlife Refuge staff, and the National Science Foundation Beaufort Lagoon Ecosystem Long Term Ecological Research program for their assistance. We would like to thank James McClelland and two anonymous reviewers whose suggestions improved this work. This work was supported by funding from the U.S. Geological Survey (USGS) Outer Continental Shelf Program and the USGS Changing Arctic Ecosystems Initiative. Any use of trade, firm, or product names is for descriptive purposes only and does not imply endorsement by the U.S. Government.

Submitted 12 January 2024
Revised 13 September 2024
Accepted 17 September 2024

23782242, 2024, 6, Downloaded from https://aslopubs.onlinelibrary.wiley.com/doi/10.1002/lol2.10442, Wiley Online Library on [13/03/2025]. See the Terms and Conditions (https://onlinelibrary.wiley.com/terms-and-conditions) on Wiley Online Library for rules of use; OA articles are governed by the applicable Creative Commons License